Enhancement of the ECMA-368 UWB System by Means of Compatible Relaying Techniques†

(Invited Paper)

Jimmy Kan[1], Jan Mietzner[2], Chris Snow[3], and Robert Schober[2]

[1] Microsoft Corporation, Internet Platform and Operations Group,
1 Microsoft Way, Redmond, WA 98052-6399, USA. E-mail: jimmy.kan@microsoft.com.

[2] University of British Columbia, Department of Electrical & Computer Engineering,
2332 Main Mall, Vancouver, BC, V6T 1Z4, Canada. E-mail: {janm,rschober}@ece.ubc.ca.

[3] Research in Motion Limited, RIM Cellular Technologies,
295 Phillip Street, Waterloo, ON, N2L 3W8, Canada. E-mail: chsnow@rim.com.

***Abstract*—We assess the benefits of relaying techniques with regard to the performance of ECMA-368 ultra wideband radio systems. To this end, we closely follow the current ECMA-368 standard and adopt the IEEE 802.15.3a channel models. Focus is on compatible relaying techniques that require a minimum of change to the current system specifications. In particular, we consider decode-and-forward (D&F) and amplify-and-forward (A&F) relaying and combine these techniques with a distributed version of cyclic delay diversity (CDD) performed across relays. Our results show that, as long as the relays are located sufficiently close to the source node, both D&F and A&F relaying achieve significant performance gains over direct transmission, even in the case of correlated shadowing. Furthermore, we find that the distributed CDD scheme yields little improvements compared to simple A&F and D&F relaying, since the employed channel coding scheme already picks up a large amount microscopic diversity.**

I. INTRODUCTION

ULTRA wideband (UWB) radio technology is currently considered one of the strongest contenders for future high-rate, short-range wireless communication systems [1]. While traditionally, spectrum usage has been organized according to fixed frequency plans defined through government licences, UWB radio constitutes a first step in the direction of unlicensed wireless communications. Recently, the first standards for UWB radio systems have been created [2],[3], and several regulatory bodies around the world have approved UWB transmission in (parts of) the 3.1-10.6 GHz band. In this paper, focus is on the ECMA-368 standard[1] [2], which currently receives strong support from the wireless industry.

In order to protect existing licensed wireless services from excessive interference, the US Federal Communications Commission (FCC) has defined a spectral mask for UWB devices [4], which limits the permitted radiated power levels to very small values (below -41.3 dBm/MHz). Due to these restrictions, the use of relaying techniques appears to be very attractive, so as to guarantee a certain quality of service for UWB radio systems and/or to extend their coverage. Surprisingly, the literature on relaying techniques for UWB radio systems is still comparatively sparse, e.g. [5]-[9]. In particular, most papers tend to neglect existing technical standards (or standard proposals) for UWB radio systems or follow them rather loosely. This might limit their relevance with regard to practical implementations. For example, the ECMA-368 standard [2] is considered in [8], but the proposed relaying techniques do not comply with the current standard, since they comprise hierarchical modulation and distributed space-time coding. Similarly, in [6] cooperative relaying schemes for UWB radio systems that are based on multiband orthogonal frequency division multiplexing (MB-OFDM) are considered. However, neither the specific channel coding schemes defined within the ECMA-368 standard nor the log-normal shadowing that is typical for UWB channels [10] are taken into account.

The objective of this paper is to provide realistic results concerning the benefits of relaying techniques with regard to the performance and coverage of ECMA-368 systems. We will therefore closely follow the current system standard and adopt the IEEE 802.15.3a UWB channel models (CMs), which include the typical clustering behavior of multipath arrivals, shadowing effects as well as realistic path-loss modeling [10]. Moreover, we will focus on compatible relaying techniques requiring a minimum of change to the current system specifications, and assess their performance for various cases. In particular, we will consider decode-and-forward (D&F) and amplify-and-forward (A&F) relaying, and investigate the use of a distributed version of cyclic delay diversity (CDD) [11] performed across relays, as a means to provide additional spatial diversity.

The remainder of this paper is organized as follows: In Section II, the system and channel model as well as the relaying techniques under consideration are discussed. In Section III, numerical performance results are presented, and the benefits of the considered relaying techniques are highlighted. Finally, concluding remarks are offered in Section IV.

II. SYSTEM MODEL AND RELAYING TECHNIQUES

We first consider a point-to-point link and give a brief description of the ECMA-368 standard and the employed UWB channel models. Afterwards, the relaying protocol and the different relaying techniques under consideration will be discussed.

1) ECMA-368 system model: The ECMA-368 standard is based on MB-OFDM [12]. The corresponding system model in complex baseband notation is shown in Fig. 1. In this paper, we consider the first generation of ECMA-368 systems, which employs three 528 MHz subbands within the 3.1-4.8 GHz band [2]. Each subband comprises $N_\mathrm{c} = 128$ orthogonal subcarriers, from which 100 subcarriers are available for data transmission and 28 subcarriers are used as guard or pilot tones. As an option, frequency-hopping (FH) can be performed between the individual subbands, so as to provide additional diversity in the frequency domain. Technically, the employed MB-OFDM scheme falls into the class of zero-padding (ZP) OFDM, as opposed to the more common cyclic-prefix (CP) OFDM. The length of the ZP part is given by $N_\mathrm{zp} = 37$. If overlap-and-add (O+A) processing is employed at the receiver and the underlying channel impulse response (CIR) is sufficiently short, a circulant overall channel matrix is obtained [13], which is then diagonalized by the (inverse) fast Fourier transform (IFFT/FFT) pair at transmitter and receiver (similar to CP-OFDM).

(a) Transmitter structure: Within the scope of this paper, we focus on the ECMA-368 data-rate modes 53.3 Mb/s, 80 Mb/s, 106.7 Mb/s, 160 Mb/s, and 200 Mb/s, which employ quadrature phase-shift-keying (QPSK) modulation with Gray map-

†This work was supported by a postdoctoral fellowship from the German Academic Exchange Service (DAAD).

[1]ECMA stands for ECMA International – European association for standardizing information and communication systems.

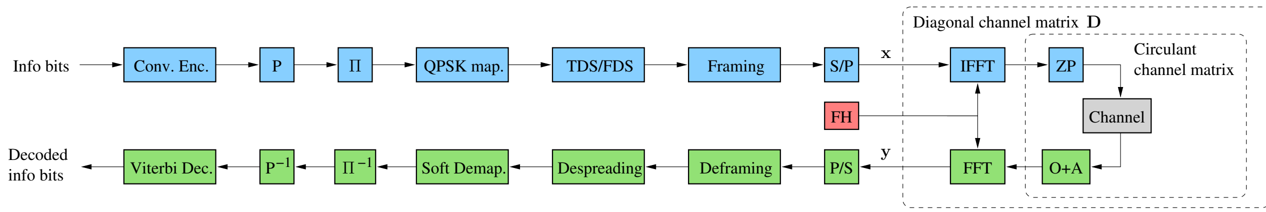

Fig. 1. MB-OFDM system model according to the ECMA-368 standard, including convolutional coding, puncturing (P), bit interleaving (Π), QPSK mapping, time-domain/frequency-domain spreading (TDS/FDS), frequency hopping (FH), and the ZP-OFDM modulation.

TABLE I
CONSIDERED DATA-RATE MODES WITHIN THE ECMA-368 STANDARD

Data Rate	Punctured Code Rate	Spreading	Bits per OFDM frame
53.3 Mb/s	$R_\mathrm{p} = 1/3$	FDS & TDS	$N_\mathrm{i} = 100$
80 Mb/s	$R_\mathrm{p} = 1/2$	FDS & TDS	$N_\mathrm{i} = 150$
106.7 Mb/s	$R_\mathrm{p} = 1/3$	TDS	$N_\mathrm{i} = 200$
160 Mb/s	$R_\mathrm{p} = 1/2$	TDS	$N_\mathrm{i} = 300$
200 Mb/s	$R_\mathrm{p} = 5/8$	TDS	$N_\mathrm{i} = 375$

ping on each subcarrier. The various data-rate modes are realized by means of suitable combinations of punctured convolutional codes, time-domain spreading (TDS), and frequency-domain spreading (FDS), see Table I. At the transmitter side, the information bits are first encoded by a rate-1/3 convolutional encoder. Then, puncturing (P) and bit interleaving (Π) are applied, followed by the QPSK symbol mapping, FDS and TDS. Finally, the resulting complex symbols are collected in a frame, and serial-to-parallel (S/P) conversion is performed to obtain the individual OFDM symbols. In the case of FDS, each QPSK symbol is transmitted over two separate subcarriers within the same OFDM symbol, while in the case of TDS the entire OFDM symbol is transmitted twice. Throughout this paper, we assume that each OFDM frame consists of six subsequent OFDM symbols. In the case of FH, the three available subbands are changed according to an 'ABCABCA...' hopping sequence, where each subband is retained for the duration of a single OFDM symbol.[2] In addition to the convolutional code, the ECMA-368 standard also comprises an outer cyclic-redundancy-check (CRC) code for error detection (not depicted in Fig. 1), which spans a complete OFDM frame. In the following, we assume that the CRC code is able to perfectly detect erroneous received OFDM frames.

(b) Receiver structure: The receiver part is not further specified in [2]. After parallel-to-serial (P/S) conversion of the received OFDM symbols, the receiver needs to perform FD/TD despreading, QPSK demapping, deinterleaving (Π^{-1}), depuncturing (P^{-1}), and convolutional decoding. In this paper, FD/TD despreading is performed by means of maximal-ratio combining (MRC) of the corresponding received QPSK symbols. Demapping is done using a soft QPSK demapper, and convolutional decoding is carried out by means of the Viterbi algorithm.

2) UWB channel model: We adopt the IEEE 802.15.3a UWB channel models CM1–CM4 [10]. Correspondingly, the passband CIR $h_i(t)$ associated with point-to-point link i consists of L_c clusters of L_r rays, and is modeled as

$$h_i(t) = X_i \sum_{l=1}^{L_\mathrm{c}} \sum_{k=1}^{L_\mathrm{r}} \alpha_{i,k,l}\, \delta(t - T_{i,l} - \tau_{i,k,l}), \tag{1}$$

where $\delta(t-t_0)$ denotes a Dirac impulse at time $t = t_0$, $T_{i,l}$ is the random delay of the lth cluster, $\tau_{i,k,l}$ is the random delay of the kth ray within the lth cluster, and $\alpha_{i,k,l}$ is the corresponding random multipath gain (see [10] for further details). Throughout this paper, we assume quasi-static fading. The outer shadowing term X_i is modeled as a log-normal random variable, i.e., $X_i \sim 10^{\sigma_x w_i/20}$, where σ_x denotes the standard deviation of the lognormal shadowing (set to $\sigma_x = 3$ for CM1–CM4 [10]) and w_i is a zero-mean, unit-variance Gaussian random variable.

[2]Alternative hopping patterns are also possible. However, the resulting system performance is similar for the different hopping patterns specified in [2].

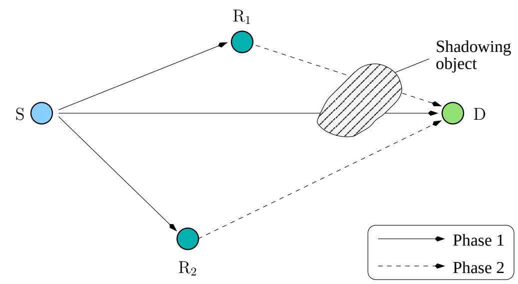

Fig. 2. Relaying setup under consideration for the case of $N_\mathrm{r} = 2$ available relays (S: source node, R_j: relay nodes, D: destination node). The shadowing object that is found close to the destination node will cause shadowing correlation between the $\mathrm{S} \to \mathrm{D}$ link and the $\mathrm{R}_1 \to \mathrm{D}$ link.

(a) Path-loss model: In the relaying case, we additionally need to employ a path-loss exponent p, so as to account for different link lengths between the source node S, the available relay nodes R_j, and the destination node D, cf. Fig. 2. According to [10], we choose $p = 1.7$ for CM1 (line-of-sight scenario) and $p = 3.5$ for CM2–CM4 (non-line-of-sight scenarios). In the following, the source-destination link will serve as the reference link, i.e., the corresponding CIR energy is normalized to one, while the CIR energies of the remaining links are normalized according to the relative link lengths.

(b) Correlated shadowing: In the relaying case, the lognormal shadowing terms X_i, $X_{i'}$ associated with different links i and i' might be correlated, i.e., $\rho_{i,i'} := \mathsf{E}\{w_i w_{i'}\} > 0$, where $\mathsf{E}\{\,.\,\}$ denotes statistical expectation [14]. This could, for example, be caused by shadowing objects that are found close to a common transmitter or a common receiver, as illustrated in Fig. 2. As opposed to this, the random delays $T_{i,l}$, $\tau_{i,k,l}$ and the random multipath gain coefficients $\alpha_{i,k,l}$ can typically be considered statistically independent across links [14].

3) Relaying protocol: We consider a two-hop relaying setup as depicted in Fig. 2. For simplicity and practical relevance, we assume that the source node S, the available relays R_j ($j = 1, ..., N_\mathrm{r}$), and the destination node D employ a single antenna. Throughout this paper, we consider a two-phase relaying protocol (cf. Fig. 2), similar to the space-time coded protocol proposed in [15]. In the first phase, the source node broadcasts an entire OFDM frame, which is received by the destination node and the available relays. The employed transmit power per subcarrier and OFDM symbol is in the sequel denoted as P. Due to the ZP-OFDM modulation, the νth received OFDM symbol $\mathbf{y}^{(1)}_{\mathrm{Y},\nu}$ at node $\mathrm{Y} \in \{\mathrm{D}, \mathrm{R}_j\}$ can be written as [13]

$$\mathbf{y}^{(1)}_{\mathrm{Y},\nu} = \mathbf{D}_{\mathrm{S,Y}}\, \mathbf{x}_\nu + \mathbf{n}^{(1)}_{\mathrm{Y},\nu}, \tag{2}$$

where $\mathbf{D}_{\mathrm{S,Y}}$ is a diagonal $(N_\mathrm{c} \times N_\mathrm{c})$-matrix with diagonal entries given by the sampled frequency response of the associated baseband CIR, $\mathbf{x}_\nu$ denotes the νth transmitted OFDM symbol, and $\mathbf{n}^{(1)}_{\mathrm{Y},\nu}$ an additive white Gaussian noise (AWGN) vector.

In the second phase, the participating relays simultaneously forward the received OFDM frame to the destination node. Note that we do not assume that the relays perform orthogonal transmissions (e.g., using orthogonal time slots). Correspondingly, the relayed signals simply add up at the destination node.

(a) D&F relaying: In the case of D&F relaying, the available relays completely decode the received OFDM frame to obtain the information bits (cf. Fig. 1). The employed outer CRC code is then exploited in order to detect possible decoding errors. Those relays which were able to decode the OFDM frame correctly, re-encode the entire frame and forward it to the destination node, while all other relays remain silent. By this means, error propagation effects are avoided, however, at the expense of a comparatively high signal processing complexity required at the relays. In the following, we assume that the active D&F relays use the same transmit power P per subcarrier and OFDM symbol as the source node.[3] Similarly to (2), the νth received OFDM symbol at the destination node during the second transmission phase can thus be written as

$$\mathbf{y}^{(2)}_{\mathrm{D},\nu} = \mathbf{D}_{\mathrm{R,D,eff}}\,\mathbf{x}_\nu + \mathbf{n}^{(2)}_{\mathrm{D},\nu}, \qquad (3)$$

where $\mathbf{D}_{\mathrm{R,D,eff}} := \sum_{j \in \mathbb{I}} \mathbf{D}_{\mathrm{R}_j,\mathrm{D}}$ and $\mathbb{I} \subseteq \{1, ..., N_\mathrm{r}\}$ denotes the index set associated with the active D&F relays.

(b) A&F relaying: In the case of A&F relaying, all available relays take part in the relaying process. Each relay takes the received time-domain signal, normalizes it according to an average transmit power constraint, and retransmits it to the destination node. Note that neither O+A processing nor any IFFT/FFT operations are required at the relays, which renders A&F relaying particularly simple. Similarly to (3), the νth received OFDM symbol at the destination node can be written as

$$\mathbf{y}^{(2)}_{\mathrm{D},\nu} = \mathbf{D}_{\mathrm{R,D,eff}}\,\mathbf{x}_\nu + \mathbf{n}^{(2)}_{\mathrm{D,eff},\nu}, \qquad (4)$$

where $\mathbf{D}_{\mathrm{R,D,eff}} := \sum_{j=1}^{N_\mathrm{r}} \alpha_j \mathbf{D}_{\mathrm{S,R}_j} \mathbf{D}_{\mathrm{R}_j,\mathrm{D}}$ and $\mathbf{n}^{(2)}_{\mathrm{D,eff},\nu} := \mathbf{n}^{(2)}_{\mathrm{D},\nu} + \sum_{j=1}^{N_\mathrm{r}} \alpha_j \mathbf{D}_{\mathrm{R}_j,\mathrm{D}} \mathbf{n}^{(1)}_{\mathrm{R}_j,\nu}$. The normalization factors α_j are chosen such that each relay R_j uses an average transmit power of P per subcarrier and OFDM symbol (similar to the D&F case). A drawback of A&F relaying is that noisy signals are forwarded to the destination node. Moreover, A&F relaying increases the effective CIR length seen at the destination node, as the overall CIR results from a convolution of the CIRs associated with the source-relay link and the relay-destination link. While for the channel models CM1 and CM2 this is typically uncritical, we found that for CM3 and CM4 the effective CIR length tends to exceed the ZP guard interval, which causes residual intersymbol interference. Finally, it might be difficult to guarantee that the FCC spectral mask is met by the relays, since at each relay the spectrum of the transmitted signal contains the (non-flat) frequency response of the corresponding source-relay channel. In practice, this problem can, for example, be solved by applying an appropriate power back-off factor at the relays. For simplicity, we will neglect this issue in the following.

(c) MRC at the destination: After completion of the two transmission phases, the destination node performs MRC of the corresponding received signals $\mathbf{y}^{(1)}_{\mathrm{D},\nu}$ and $\mathbf{y}^{(2)}_{\mathrm{D},\nu}$. To this end, we assume that the entries of the matrices $\mathbf{D}_{\mathrm{S,D}}$ and $\mathbf{D}_{\mathrm{R,D,eff}}$ are perfectly known at the destination. In practice, they need to be estimated using an appropriate channel estimation scheme. Finally, we note that in the case of A&F relaying the MRC step needs to take the unequal noise variances associated with the noise vectors $\mathbf{n}^{(1)}_{\mathrm{D},\nu}$ and $\mathbf{n}^{(2)}_{\mathrm{D,eff},\nu}$ into account.

(d) Rate loss: Note that the employed relaying protocol entails a rate loss of factor $1/2$ compared to direct transmission. We will account for this by considering the data-rate modes 106.7 Mb/s and 160 Mb/s in the case of relaying and compare them to direct transmission at data rates of 53.3 Mb/s and 80 Mb/s, respectively.

4) Distributed CDD: In order to provide additional (microscopic) diversity in the spatial domain, the participating relays can employ a distributed space-time coding scheme, e.g., [5], [8], [15]. In this paper we focus on CDD, which was originally developed for CP-OFDM systems with multiple co-located transmit antennas [11], and combine it with D&F and A&F relaying. In conventional CDD, each transmit antenna applies a (unique) cyclic shift to the transmitted OFDM symbol (after the IFFT). By this means, the effective frequency diversity of the channel is increased, which can then be picked up by an outer channel coding scheme. CDD does not increase the effective channel memory length. Another advantage of CDD is that it is transparent to the receiver and the channel estimation process, i.e., the receiver structure does not have to be modified at all. In particular, the cyclic shifts employed at the transmitter side do not need to be known at the receiver.

We first note that CDD can also be applied in ZP-OFDM systems with O+A processing at the receiver, due to the resulting circulant channel matrix. Secondly, in order to have a distributed CDD scheme across active relays, we consider the case that each relay employs a random cyclic shift, so that no further signaling between the relays is required. Similar to the case of co-located antennas, we can thus increase the effective frequency diversity of the system, while retaining the receiver structure at the destination node.

Finally, we note that the cyclic shift at the relays has to be performed after the O+A processing. If CDD is employed, we therefore need to modify the above A&F relaying scheme such that O+A processing (and insertion of a new ZP part) is performed at the relays, which will slightly increase the signal processing complexity.

III. Numerical Performance Results

In this section, the benefits of D&F relaying, A&F relaying, and distributed CDD with regard to the performance and coverage of ECMA-368 systems are assessed based on numerical performance results. Moreover, the impact of path-loss effects, relay positions, and shadowing effects on the overall system performance will be illustrated.

Throughout this section, we assume that up to $N_\mathrm{r} = 2$ relays are available, having fixed positions between the source and the destination node (cf. Fig. 2). The (average) transmitted symbol energy per subcarrier and OFDM symbol at the source node and each relay is in the following denoted as $E_\mathrm{s} := PT_\mathrm{s}/(N_\mathrm{c} + N_\mathrm{zp})$, where T_s denotes the duration of an OFDM symbol (including the ZP part). The positions of the source node and the destination node are in the following set to $(-0.5, 0)$ and $(+0.5, 0)$, respectively. If not stated otherwise, the relay positions are set to $(0, 0)$ in the case of $N_\mathrm{r} = 1$ relay and to $(0, \pm 0.1)$ in the case of $N_\mathrm{r} = 2$ relays. All numerical performance results presented below were obtained by means of Monte-Carlo simulations over a sufficiently large number of OFDM frames. The resulting average bit error rates (BERs) are displayed versus E_b/N_0 in dB, where E_b denotes the overall average energy per information bit transmitted by the source and the relay node(s), and N_0 denotes the single-sided power spectral density of the underlying passband AWGN process. The noise statistics at the destination

[3]The numerical performance results presented later on in Section III have been normalized accordingly, so as to provide a fair comparison between the relaying case and the case of direct transmission.

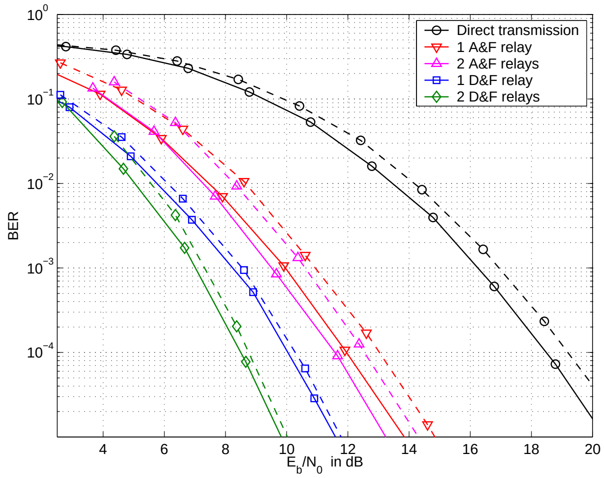

Fig. 3. Performance of D&F and A&F relaying for channel model CM2 and uncorrelated shadowing (no FH); data-rate modes 160 Mb/s (solid lines) and 106.7 Mb/s (dashed lines) in comparison with direct transmission with data-rate modes 80 Mb/s (solid lines) and 53.3 Mb/s (dashed lines), respectively.

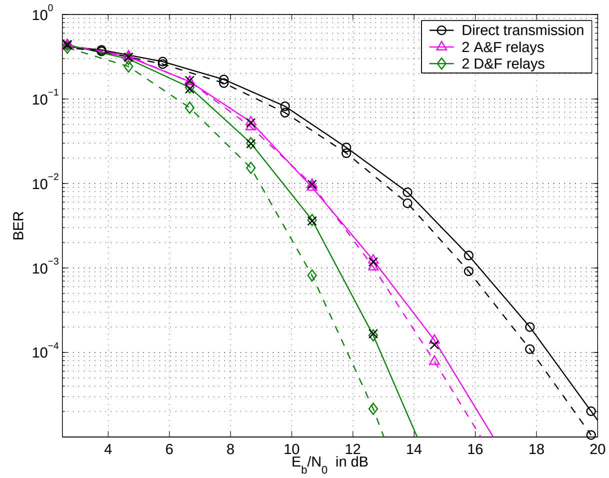

Fig. 4. Performance of D&F and A&F relaying for channel model CM1 and uncorrelated shadowing; data-rate mode 160 Mb/s in comparison with direct transmission with data-rate mode 80 Mb/s. Dashed lines: with FH; markers 'x': with CDD (no FH).

node and all relay nodes are assumed identical. Based on Table I, the overall average transmitted bit energy E_b for the different data-rate modes is calculated as

$$E_\mathrm{b} = \frac{N_\mathrm{i} - 8}{N_\mathrm{i}} \cdot \frac{1}{R_\mathrm{p}} \cdot \frac{n}{2} \cdot (N_\mathrm{r} + 1) \cdot E_\mathrm{s}. \tag{5}$$

Here, N_i denotes the number of bits per OFDM frame (cf. Table I), from which 8 bits are used as tailing bits for the convolutional encoder, R_p denotes the rate of the punctured convolutional code, the factor n takes the FDS and TDS into account, where $n = 4$ for data-rate modes 53.3 Mb/s and 80 Mb/s and $n = 2$ for the remaining data-rate modes, the factor 1/2 takes the QPSK modulation into account, and the factor $(N_\mathrm{r} + 1)$ takes the number of available relays into account, so as provide a fair comparison between the relaying case and the case of direct transmission.

Fig. 3 shows performance results for D&F and A&F relaying in comparison with direct transmission for $N_\mathrm{r} = 1$ and $N_\mathrm{r} = 2$ relays, IEEE 802.15.3a UWB channel model CM2 ($p = 3.5$), and uncorrelated shadowing between all links. FH was not applied. For the relaying case, the data-rate modes 106.7 Mb/s and 160 Mb/s have been considered and for direct transmission the comparable data-rate modes 53.3 Mb/s and 80 Mb/s, respectively. As can be seen, both D&F and A&F relaying provide significant performance improvements over direct transmission, for the lower data-rate modes (dashed lines) as well as for the higher data-rate modes (solid lines). For example, for the higher data-rate modes, a single D&F relay provides a gain of about 8.5 dB over direct transmission (at a BER of 10^{-4}), while a single A&F relay provides a gain of about 6.5 dB. Given the value of the path-loss exponent p, this translates into an effective range extension of 75% in the case of the D&F relay and 53% in the case of the A&F relay. Obviously, D&F relaying significantly outperforms A&F relaying. This is because D&F relaying effectively uses the employed channel coding schemes for error correction at the relays, along with the microscopic frequency diversity acquired through the bit interleaving.[4] Due to the same reason, a second D&F relay yields further significant improvements compared to a single D&F relay (about 1.5 dB at a BER of 10^{-4}). As opposed to this, the performance gains achievable with A&F relaying are mainly due to path-loss and macroscopic diversity gains, and are essentially captured already by a single A&F relay.[5] However, as discussed earlier, the performance advantages of D&F relaying come at the expense of a significantly higher relay complexity. Finally, note that in all considered cases the higher data-rate mode exhibits a (slightly) better performance than the lower data-rate mode, which is partly due to the first factor $(N_\mathrm{i} - 8)/N_\mathrm{i}$ in the calculation of E_b, cf. (5) and Table I.

Fig. 4 shows corresponding performance results for channel model CM1 ($p = 1.7$), $N_\mathrm{r} = 2$ relays, and the data-rate modes 160 Mb/s and 80 Mb/s (solid lines). Performance results for the case of FH (dashed lines) and distributed CDD (markers 'x') have also been included. We first note that direct transmission offers a similar performance as in the case of channel model CM2. Moreover, in terms of E_b/N_0 both A&F and D&F relaying offer smaller performance gains over direct transmission than in the case of channel model CM2, due to the reduced path-loss gains. For example, at a BER of 10^{-4} D&F relaying provides a gain of about 5.5 dB over direct transmission and A&F relaying a gain of about 3.5 dB. Yet, given the value of the path-loss exponent p, this translates into an effective range extension of 110% in the case of D&F relaying and 61% in the case of A&F relaying. As can be seen, FH yields additional performance gains of 0.5 dB in the case of direct transmission, 0.3 dB in the case of A&F relaying, and 1.2 dB in the case of D&F relaying.[6] Finally, we observe that the distributed CDD scheme offers virtually no additional gains, neither for D&F nor A&F relaying.[7] This means that the employed channel coding scheme already picks up a large amount of microscopic diversity in the frequency domain (mainly due to the employed bit interleaving), so that the increased frequency diversity offered by the distributed CDD scheme yields little improvement.

In Fig. 5, the performance of D&F and A&F relaying is assessed for the case of $N_\mathrm{r} = 1$ relay with different positions $(x, 0)$. Similarly to Fig. 3, channel model CM2 ($p = 3.5$) with uncorrelated shadowing between all links is considered. Focus is again on the data-rate modes 160 Mb/s and 80 Mb/s. As

[4] In an uncoded system, D&F relaying is not necessarily superior to A&F relaying, see e.g. [16].

[5] Recall that due to the normalization in (5), the overall (average) transmit power is fixed and does not depend on the number of available relays. Therefore, the relative performance gains in Fig. 3 achieved by employing a second A&F relay are solely due to macroscopic diversity.

[6] Since the lognormal shadowing affects all subbands simultaneously, the observed performance gains due to FH are comparatively small. Without shadowing, we have found that FH typically offers significantly larger gains.

[7] We have made the same observations in the absence of shadowing.

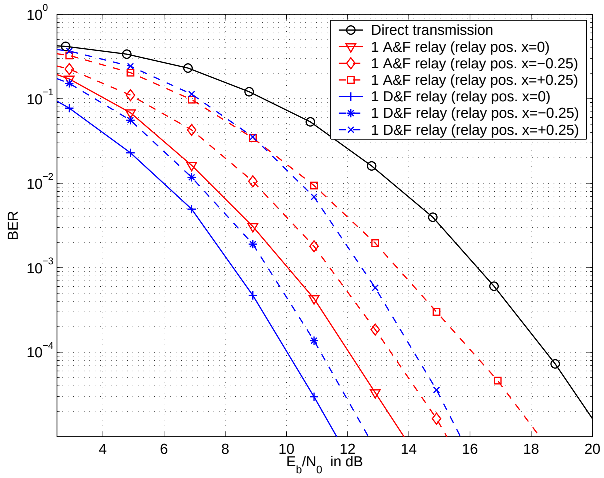

Fig. 5. Performance of D&F and A&F relaying for channel model CM2 and uncorrelated shadowing; data-rate mode 160 Mb/s in comparison with direct transmission with data-rate mode 80 Mb/s; different relay positions (no FH).

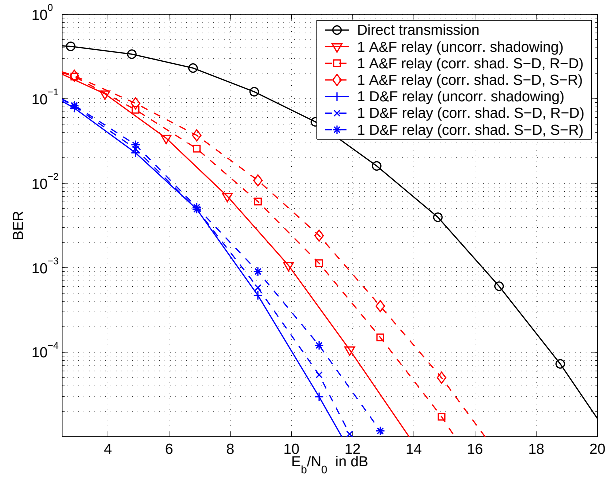

Fig. 6. Performance of D&F and A&F relaying for channel model CM2; data-rate mode 160 Mb/s in comparison with direct transmission with data-rate mode 80 Mb/s; uncorrelated shadowing vs. correlated shadowing (no FH).

can be seen, a relay position midway between source and destination node ($x=0$, solid lines) leads to the best performance among the considered cases. If the relay is located closer to the source node ($x=-0.25$), D&F and A&F relaying still achieve substantial performance gains over direct transmission. However, a relay position closer to the destination node entails a considerable performance degradation, as the D&F relay is less often able to correctly decode the received OFDM frame and the A&F relay entails larger noise enhancement.

Finally, in Fig. 6 the performance of D&F and A&F relaying is assessed for the case of correlated shadowing ($\rho_{i,i'} := 0.9$). Focus is on $N_\mathrm{r}=1$ relay with position $(0,0)$, channel model CM2 ($p=3.5$), and the data-rate modes 160 Mb/s and 80 Mb/s. As expected, the best performance is obtained when the individual links are subject to uncorrelated lognormal shadowing (solid lines). Correlated shadowing between the source-destination link $\mathrm{S} \rightarrow \mathrm{D}$ and the relay-destination link $\mathrm{R} \rightarrow \mathrm{D}$ or between the $\mathrm{S} \rightarrow \mathrm{D}$ link and the source-relay link $\mathrm{S} \rightarrow \mathrm{R}$ entails some performance degradations (especially in the case of A&F relaying), while the latter case is less favorable in this example. Still, significant performance improvements over direct transmission are achieved in all considered cases.

IV. Concluding Remarks

In this paper, the benefits of D&F and A&F relaying techniques with regard to the performance and coverage of ECMA-368 UWB systems have been considered. In order to provide realistic performance results, we have closely followed the current system standard and have adopted the IEEE 802.15.3a UWB channel models. Moreover, we have focussed on compatible relaying techniques that require a minimum of change to the current system specifications. Our results have shown that, as long as the relays are located sufficiently close to the source node, both D&F and A&F relaying achieve significant performance gains over direct transmission, even if the individual links are subject to correlated shadowing. Furthermore, we have investigated the benefits of a distributed CDD scheme across the relays, so as to provide additional spatial diversity. We have found that the distributed CDD scheme yields little improvements, since the employed channel coding scheme already picks up a large amount microscopic diversity in the frequency domain. More generally, this result implies that the use of distributed space-time coding schemes in UWB radio systems, which are able to efficiently extract the frequency diversity of the underlying channel, might be of limited value in practice. Future work might focus on more efficient, yet simple relaying schemes that can easily be guaranteed to comply with the FCC spectral mask.

References

[1] S. Roy, J. R. Foerster, V. S. Somayazulu, and D. G. Leeper, "Ultra-wideband radio design: The promise of high-speed, short-range wireless connectivity," *Proc. IEEE*, vol. 92, no. 2, pp. 295–311, Feb. 2004.

[2] "Standard ECMA-368: High rate ultra wideband PHY and MAC standard," ECMA, First Edition, Dec. 2005.

[3] "Part 15.4: Wireless medium access control (MAC) and physical layer (PHY) specifications for low-rate wireless personal area networks (LR-WPANs): Amendment to add alternate PHY," IEEE P802.15–TG4a, Jan. 2007.

[4] "Revision of part 15 of the commission's rules regarding ultra-wideband transmission systems," Federal Communications Commission (FCC), First Report and Order, ET Docket 98–153, FCC 02–48; Adopted: February 2002; Released: March 2003.

[5] X. Zhou, H. Zhang, and I. Chlamtac, "Space-frequency coded cooperative scheme among distributed nodes in cognitive UWB radio," in *Proc. IEEE Int. Symp. on Pers., Indoor, and Mobile Radio Commun. (PIMRC)*, Berlin, Germany, Sept. 2005, pp. 461–465.

[6] W. P. Siriwongpairat, A. K. Sadek, and K. J. R. Liu, "Bandwidth-efficient OFDM cooperative protocol with applications to UWB communications," in *Proc. IEEE Wireless Commun. and Networking Conf. (WCNC)*, Las Vegas, NV, USA, Apr. 2006, pp. 1729–1734.

[7] C. Abou-Rjeily, N. Daniele, and J.-C. Belfiore, "On the decode-and-forward cooperative diversity with coherent and non-coherent UWB systems," in *Proc. IEEE Int. Conf. on Ultra-Wideband (ICUWB)*, Waltham, MA, USA, Sept. 2006, pp. 435–440.

[8] J.-H. Kim and H.-K. Song, "Performance improvement of cooperative MB-OFDM system based coming home network," *IEEE Trans. Consumer Electron.*, vol. 53, no. 2, pp. 442–447, May 2007.

[9] S. Zhu and K. K. Leung, "Cooperative orthogonal MIMO-relaying for UWB ad-hoc networks," in *Proc. IEEE Global Telecommun. Conf. (Globecom)*, Washington, DC, USA, Nov. 2007, pp. 5175–5179.

[10] A. F. Molisch, J. R. Foerster, and M. Pendergrass, "Channel models for ultrawideband personal area networks," *IEEE Wireless Commun.*, vol. 10, no. 6, pp. 14–21, Dec. 2003.

[11] G. Bauch and J. S. Malik, "Cyclic delay diversity with bit-interleaved coded modulation in orthogonal frequency division multiple access," *IEEE Trans. Wireless Commun.*, vol. 5, no. 8, pp. 2092–2100, Aug. 2006.

[12] A. Batra, J. Balakrishnan, G. R. Aiello, J. R. Foerster, and A. Dabak, "Design of a multiband OFDM system for realistic UWB channel environments," *IEEE Trans. Microwave Theory Tech.*, vol. 52, no. 9, pp. 2123–2138, Sept. 2004.

[13] Z. Wang and G. B. Giannakis, "Wireless multicarrier communications – Where Fourier meets Shannon," *IEEE Signal Processing Mag.*, vol. 17, no. 3, pp. 29–48, May 2000.

[14] Z. Lin, X. Peng, K. Png, and F. Chin, "Kronecker modelling for correlated shadowing in UWB MIMO channels," in *Proc. IEEE Wireless Commun. and Networking Conf. (WCNC)*, Hong Kong, Mar. 2007, pp. 1585–1589.

[15] J. N. Laneman and G. W. Wornell, "Distributed space-time-coded protocols for exploiting cooperative diversity in wireless networks," *IEEE Trans. Inform. Theory*, vol. 49, no. 10, pp. 2415–2425, Oct. 2003.

[16] B. Can, H. Yomo, and E. De Carvalho, "Hybrid forwarding scheme for cooperative relaying in OFDM based networks," in *Proc. IEEE Int. Conf. Commun. (ICC)*, Istanbul, Turkey, June 2006, pp. 4520–4525.